



COMPUTER VISUALIZATION OF STRUCTURED LASER RADIATION REFRACTOGRAMS

M. S. KUZMICHEVA^{1c}, I. L. RASKOVSKAYA¹

¹Department of Physics named of V.A.Fabrikant, National Research University «Moscow Power Engineering Institute»,
Moscow, 111250, Russia

^cCorresponding author: Tel.: +7(495)3627755; Fax: +7(495)3628938; Email: m_s_h@mail.ru

KEYWORDS:

Main subjects: physical processes in liquid visualization

Fluid: convection, salt stratification

Visualization method(s): laser refraction method, computer modeling

Other keywords: structured laser radiation, refractography, diffraction

ABSTRACT: For experimental research of physical processes in liquids and gases can be used the method of laser refractography consisting in probe the medium of interest with structured laser radiation, record the radiation passing through the medium with a CCD camera, and process with the aid of a computer the refraction patterns captured with a view to finding out the properties of the medium. Refractograms are simulated by solving equations of geometric optics as applied to inhomogeneous mediums. However, presence a complex beam pattern in the medium, formation of caustics and need to consider the diffraction effects, geometrical optics approach is untenable and requires wave methods using.

For this purpose the authors developed a method of calculating laser refractograms based on solving wave equation. Calculating refractograms in relation of geometrical optics and Fresnel diffraction have problems associated with the requirement of large computational resources because of rapidly oscillating function under the integral sign. This paper is devoted to the implementation of the algorithm in the programming environment Delphi, which reduces the calculation time. The typical laser refractograms are shown calculated for the plane and linearly-structured laser radiation propagated through cylindrical and planar inhomogeneous layers.

The simulation results can be used in laser diagnostics of optically transparent inhomogeneous media.

1 LASER REFRACTOGRAPHY TECHNIQUE

The active application of laser techniques to the diagnostics of acoustic pressure, temperature, density, salinity, and current velocity fields in transparent media is due to their substantial advantages over other methods. First and foremost, optical measurements do not disturb the fields under study because the energy absorbed by the medium of interest is in most cases rather low, which allows diagnosing fast processes. An additional merit of laser techniques is the possibility they provide for taking remote measurements. Laser techniques make it possible to study refractive index fields that can then be converted into the desired fields of other physical quantities [1].

Laser refractography is a novel laser technique for diagnosing optically inhomogeneous media [2-4], based on the probing of the medium under study with a structured laser radiation, the digital recording of the refraction pattern (refractogram), and its computer processing with a view to recovering the properties of the medium. Regularly structured laser radiation is formed directly at the exit from the radiation source by means of special optical elements that allow the radiation to retain its high coherence and provide for low beam divergence. This makes it possible to describe structured laser radiation in terms of geometrical (ray) optics. Within the framework of ray optics, structured laser radiation can be represented by families of rays forming surfaces in the form of discrete sets of planes, nested cylinders, cones, etc.

Structured laser radiation (SLR) is a spatially amplitude-modulated radiation obtained with the aid of the classical optical elements, diffraction optical elements, or structured screens.



The main types of structured laser radiation are presented in Fig. 1. They are classed by the shape of the spatial geometrical figures formed by the rays from the source as follows: line-structured, plane-structured, and cone-structured laser radiation. The two-dimensional figures presented in the table are cross-sections of the beams formed by the families of geometrical-optics rays from the source.

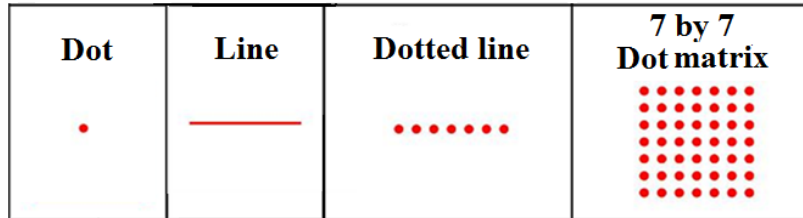


Fig.1 Main types of structured laser radiation

Obviously the initial beam structure described by a number of informative parameters changes upon the refraction of the beam in an optical inhomogeneity, which allows the inhomogeneity to be quantitatively diagnosed and visualized on the basis of the experimental refractograms.

Fig. 2 presents a block diagram of a laser refractographic system.

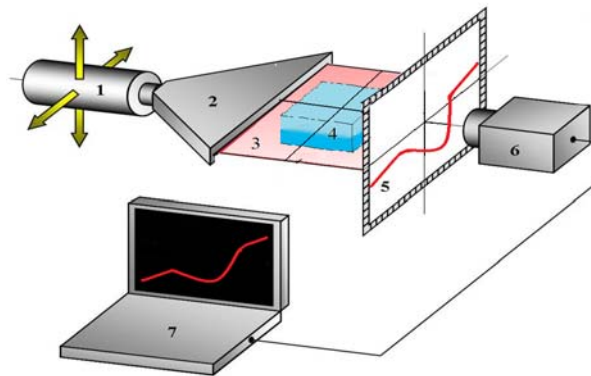


Fig. 2 Block diagram of a laser refractographic system: 1 – laser; 2 – optical SLR forming unit; 3 – SLR (laser plane); 4 – optical inhomogeneity under study; 5 – ground glass screen; 6 – digital video camera; 7 – personal computer

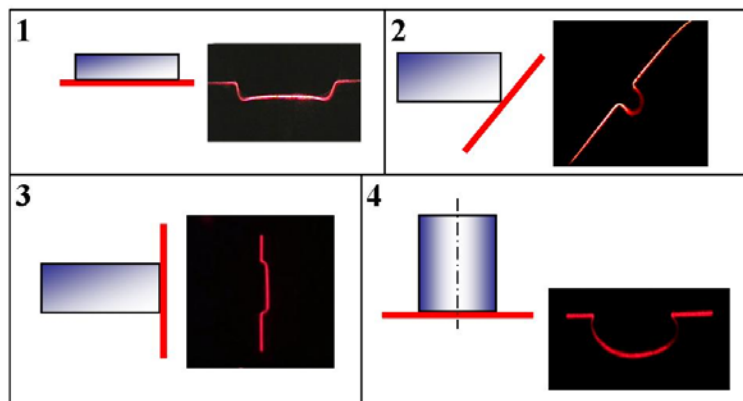


Fig. 3 Typical of experimental refractograms: 1 – horizontal laser plane beneath the bottom of a parallelepiped; 2 – inclined laser plane near an edge of a parallelepiped; 3 – vertical laser plane next to a side face of a parallelepiped; 4 – horizontal laser plane beneath the bottom of a cylinder

The mathematical modeling of the refraction patterns (refractograms) obtained by probing the medium under study with a structured laser radiation is fundamental to the quantitative diagnostics of the medium.



Geometrical-optics models of refractograms have been used to solve inverse problems on the recovery of the refractive index, temperature, and salinity of various media. However, where complex ray patterns are present or caustic surfaces are formed in the medium, or else where diffraction effects must be taken into consideration, the geometrical-optics approach proves inconsistent, and so use should be made of wave methods. For this reason, we have developed a wave-equation-based refractogram processing algorithm.

2 WAVE METHODS IN LASER REFRACTOGRAPHY PROBLEMS

2.1

In accordance with Fig. 4, the propagation of a structured laser beam probing an inhomogeneity should be modeled in the following three sections: in the free region of length l_0 from the radiation source to the inhomogeneity, within the inhomogeneity of length l_1 , and in the free region of length l from the inhomogeneity to the observation plane (the screen whereon the experimental refraction pattern is observed). In the starting formulation of the problem, we will assume that the optical field at the entry to the inhomogeneity is wholly determined by the known characteristics of the beam from the structured radiation source. Therefore, the problem is reduced to the consideration of the beam propagation straight in the inhomogeneous medium and in the region from the exit from the medium to the observation plane.

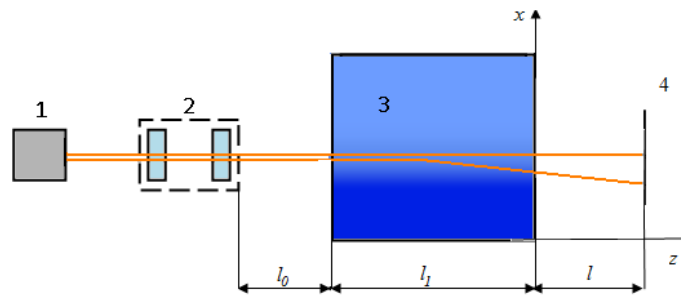


Fig. 4 Propagation of a structured laser beam probing an inhomogeneity from the radiation source to the observation plane: 1 – laser; 2 – optical SLR forming system; 3 – inhomogeneous medium; 4 – screen in the observation plane

The propagation of a beam in an inhomogeneous medium is described by the Helmholtz equation

$$\Delta U + k^2(x, y, z)U = 0. \quad (1)$$

The propagation of the structured beam in free space can be modeled on the basis of a spectral method or with the use of a Green formula.

Consider the solution of equation (1) in the case of free space, i.e., at $k(r) = k_0 = 2\pi/\lambda$.

Let the wave front at the boundary $z = 0$ corresponding to the beam exit plane of the inhomogeneity be given by

$$U(x, y, z)|_{z=0} = U_0(x, y). \quad (2)$$

Given boundary conditions (2), it is necessary to find $U(x, y, z)$ for the given z (for example, in the observation (screen) plane $z = z_s$).

2.2 Spectral Method

We represent the sought-for field $U(x, y, z)$ in the form of a two-dimensional Fourier integral (a superposition of plane waves):



$$U(x, y, z) = \frac{1}{4\pi} \iint F(k_x, k_y, z) \exp[i(k_x x + k_y y)] dk_x dk_y, \quad (3)$$

where k_x and k_y are the projections of the wave vector corresponding to a partial plane wave in the spatial spectrum F of the field.

The complex amplitude defined by expression (3) must satisfy Helmholtz equation (1) at $k = k_0$. Suffice it to require that the integrand $F(k_x, k_y, z) \exp[i(k_x x + k_y y)]$ should also satisfy this equation (by virtue of its being linear). Substituting this function into the Helmholtz equation for the homogeneous medium

$$\Delta U + k_0 U = 0, \quad (4)$$

we get

$$\frac{d^2 F}{dz^2} + (k_0^2 - k_x^2 - k_y^2) F = 0. \quad (5)$$

The boundary condition for equation (5) is

$$F(k_x, k_y, z) \Big|_{z=0} = F_0(k_x, k_y),$$

where $F_0(k_x, k_y)$ is the spatial spectrum of the field $U_0(x, y)$ in the plane $z = 0$ (at the exit from the inhomogeneity):

$$F_0(k_x, k_y) = \iint U_0(x, y) \exp[-i(k_x x + k_y y)] dx dy. \quad (6)$$

The general solution of equation (4) has the form

$$F(k_x, k_y, z) = C_1 \exp\left[i\sqrt{k^2 - k_x^2 - k_y^2} z\right] + C_2 \exp\left[-i\sqrt{k^2 - k_x^2 - k_y^2} z\right]. \quad (7)$$

The coefficient $C_2 = 0$ because there are no "reflected" waves in the half-space $z > 0$ free from wave sources. In that case,

$$F(k_x, k_y, z) = F_0(k_x, k_y) \exp\left[i\sqrt{k^2 - k_x^2 - k_y^2} z\right], \quad (8)$$

where the factor

$$H(k_x, k_y, z) = e^{i\sqrt{k^2 - k_x^2 - k_y^2} z}$$

determines the phase incursion of each plane wave during its propagation from the plane $z = 0$ to the plane $z = \text{const}$. The function $H(k_x, k_y, z)$ is sometimes referred to as the frequency characteristic of free space, with k_x and k_y being called space frequencies.

2.3 Green Formula

It frequently proves convenient to directly use the relationships between complex amplitudes – functions of coordinates – instead of spectral relation (3).

The change-over from the spectral description

$$F(k_x, k_y) = F_0(k_x, k_y) H(k_x, k_y) \quad (9)$$

to a field description can be achieved through convolution:



$$U(x, y) = \iint U_0(\xi, \eta) h(x - \xi, y - \eta) d\xi d\eta, \quad (10)$$

where the limits of integration are determined by the structure of the beam and $h(x, y)$ is related to $H(k_x, k_y)$ by the inverse Fourier transform:

$$\begin{aligned} h(x, y) &= \frac{1}{4\pi^2} \iint H(k_x, k_y) \exp[i(k_x x + k_y y)] dk_x dk_y = \\ &= \frac{1}{4\pi^2} \iint \exp\left(i\sqrt{k_0^2 - k_x^2 - k_y^2} z\right) \exp[i(k_x x + k_y y)] = -\frac{1}{2\pi} \frac{d}{dz} \left(\frac{e^{ik_0 R}}{R} \right), \end{aligned} \quad (11)$$

where $R = \sqrt{(x - \xi)^2 + (y - \eta)^2 + z^2}$.

Relation (11) follows from the Weyl formula for the expansion of a spherical wave into plane waves:

$$\frac{e^{ik_0 R}}{R} = \frac{i}{2\pi} \iint \frac{\exp\left(i\sqrt{k_0^2 - k_x^2 - k_y^2} z\right)}{\sqrt{k_0^2 - k_x^2 - k_y^2}} \exp[i(k_x x + k_y y)] dk_x dk_y. \quad (12)$$

Finally we get

$$U(x, y, z) = -\frac{1}{2\pi} \iint U_0(\xi, \eta) \frac{d}{dz} \frac{e^{ik_0 R}}{R} d\xi d\eta. \quad (13)$$

We find the derivative with respect to z :

$$\frac{d}{dz} \frac{e^{ik_0 R}}{R} = \frac{e^{ik_0 R}}{R} \left(ik_0 - \frac{1}{R} \right) \frac{dR}{dz}. \quad (14)$$

In conditions of a physical experiment, practically always $R \gg \lambda$ (wave zone), and so we can neglect the second term in parentheses to get

$$h(x, y) = \frac{1}{i\lambda} \frac{e^{ikR}}{R} \frac{dR}{dz} = \frac{1}{i\lambda} \frac{e^{ikR}}{R} \frac{z}{R}, \quad (15)$$

$$U(x, y, z) = \frac{1}{i\lambda} \iint U_0(\xi, \eta) \frac{ze^{ik_0 R}}{R^2} d\xi d\eta. \quad (16)$$

The value of $U_0(\xi, \eta)$ at the exit from the inhomogeneity can be found in the phase screen approximation, provided that the spatial dependence of the refractive index, $n(x, y)$, and the length of the inhomogeneity, l , are known. Let the field of the beam at the entry to the inhomogeneity be given by $A(x, y)$. In that case,

$$U_0(x, y) = A(x, y) \exp[ikn(x, y)l]. \quad (17)$$

Finally the field in the observation (screen) plane z_s is

$$U(x, y, z_s) = \frac{1}{i\lambda} \iint A(\xi, \eta) \exp[ik_0 n(\xi, \eta)l] \frac{ze^{ik_0 R}}{R^2} d\xi d\eta. \quad (18)$$



3 REFRACTOGRAM PROCESSING ALGORITHM

The processing of refractograms in the domain of applicability of geometrical optics and in the Fresnel diffraction region involves problems associated with the need for substantial computational resources because of the presence of a fast oscillating function in the integrand. In this connection, a special algorithm has been developed to increase the computation speed. At the base of the algorithm are numerical integration techniques, specifically the rectangle (cell) method.

Consider the double integral over the rectangle $G(a \leq x \leq b, \alpha \leq y \leq \beta)$ (Fig.5).

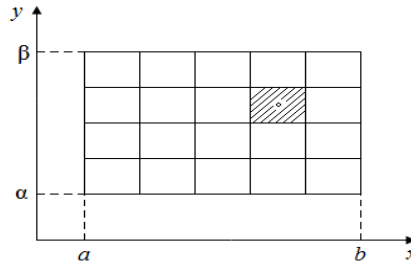


Fig. 5 Region of integration

The integrand can approximately be replaced by its value at the central point of the rectangle. In that case, the integral is easy to compute:

$$\int_a^b \int_\alpha^\beta f(x, y) dx dy \approx Sf(\bar{x}, \bar{y}), \quad (19)$$

where $S = (b - a)(\beta - \alpha)$, $\bar{x} = \frac{1}{2}(a + b)$, $\bar{y} = \frac{1}{2}(\alpha + \beta)$.

To improve accuracy, the region can be divided into rectangular cells. Approximately computing the integral over each cell and denoting by S_i and \bar{x}_i, \bar{y}_i the surface area and coordinates of the i th rectangle, respectively, we get

$$I = \iint_G f(x, y) dx dy \approx \sum_i S_i f(\bar{x}_i, \bar{y}_i). \quad (20)$$

On the right-hand side there is an integral sum; consequently, for a continuous $f(x, y)$ it converges to the value of the integral as the cell perimeters tend to zero.

This method of integration has been implemented in the *Delphi* programming environment. The appearance of this program is presented in Fig. 6.

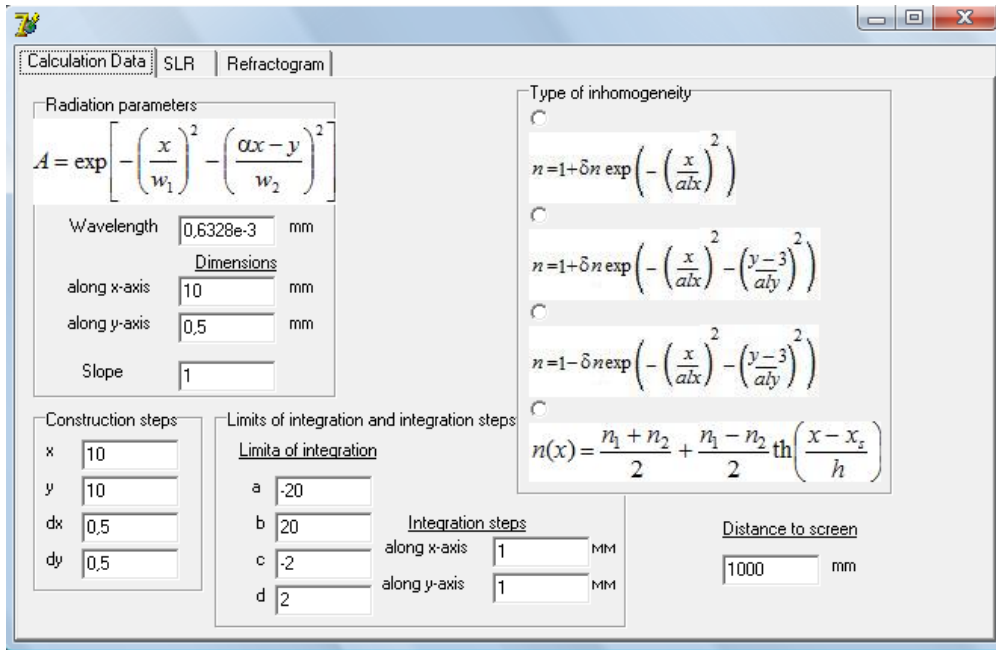


Fig. 6 Appearance of the "Refractogram" program

The program contains three panels serving to enter (select) calculation data and to display the images of the structured laser radiation used and the refractogram obtained in the observation plane. The radiation at the entry to the inhomogeneity is described by formula (21):

$$A(x, y) = \exp \left[- \left(\frac{x}{w_1} \right)^2 - \left(\frac{\alpha x - y}{w_2} \right)^2 \right], \quad (21)$$

where w_1 and w_2 stand for the dimension of the radiation along the x - and y -axes, respectively, and α is the slope of the laser plane.

It is necessary to select the type of inhomogeneity. When one of the first three types of inhomogeneity is selected, there pops up a window serving to enter the inhomogeneity parameters (Fig. 7).

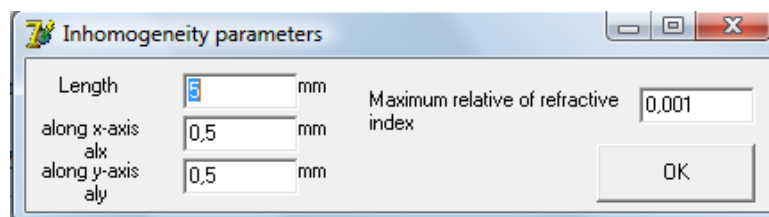


Fig. 7 Inhomogeneity parameter selection window

When selecting the fourth type of inhomogeneity that corresponds to a diffuse layer formed between two dissimilar liquids, the window shown in Fig. 8 pops up.

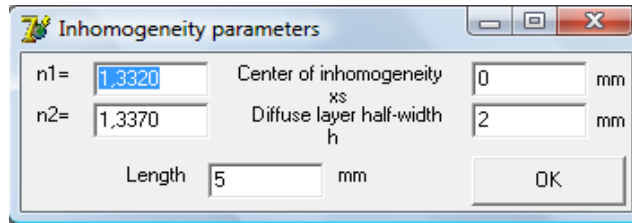


Fig. 8 Inhomogeneity parameter selection window

It is also necessary to enter the distance at which the refraction pattern is observed, the integration steps and limits of integration, as well as the steps needed to graphically represent the data.

4 RESULTS OF COMPUTER VISUALIZATION

Starting data

$\lambda = 0.6328 \times 10^{-3}$ mm;
 $w_1 = 30$ mm;
 $w_2 = 0.5$ mm.

Results of Operation of the Program

1) The law of variation of the refractive index is

$$n(y) = \frac{n_1 + n_2}{2} + \frac{n_1 - n_2}{2} \operatorname{th} \left(\frac{y - y_s}{h} \right),$$

where

$n_1 = 1.3320$ is the refractive index of the top layer;
 $y_s = 0$ is the position of the center of the inhomogeneity;
 $h = 2$ mm is the half-width of the diffuse layer.

a) *Form of refractogram as a function of the refractive index n_2 of the bottom layer*

$\alpha = 0.5$ is the laser plane slope;
 $l = 5$ mm is the length of the inhomogeneity.
 $z = 3000$ mm is the distance between the inhomogeneity and the screen.

Radiation at the entry to the inhomogeneity has the form shown in Fig. 9.

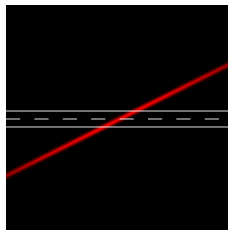
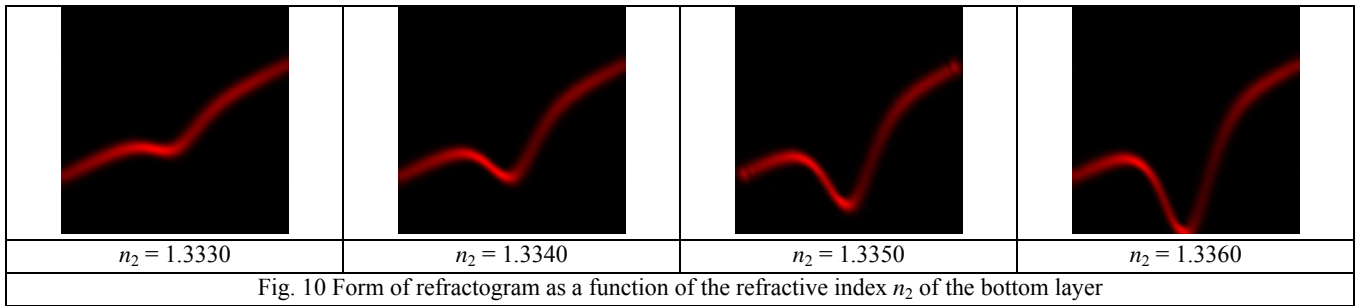


Fig. 9 Radiation at the entry to the inhomogeneity



b) Form of refractogram as a function of the distance z to the screen.
 $\alpha = 0.5$;
 $n_2 = 1.3350$.

Radiation at the entry to the inhomogeneity has the form shown in Fig. 11.

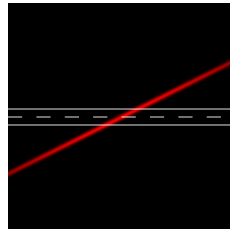
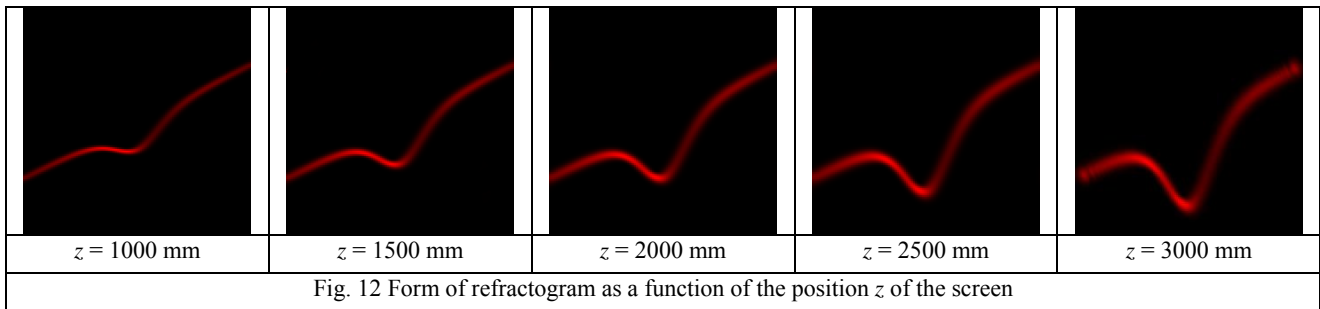


Fig. 11 Radiation at the entry to the inhomogeneity



2) The law of variation of the refractive index is

$$n = 1 - \delta n \exp\left(-\left(\frac{x}{alx}\right)^2 - \left(\frac{y-3}{aly}\right)^2\right),$$

which corresponds to a cylindrical inhomogeneity with a negative refractive index gradient.;
 $l = alx = aly = 5 \text{ mm}$ is the length of the inhomogeneity and its characteristic dimensions along the x - and y -axes;
 $\delta n = 0,002$ is the maximum relative change of the refractive index.

The laser plane slope is $\alpha = 0$.



Radiation at the entry to the inhomogeneity has the form shown in Fig. 13.

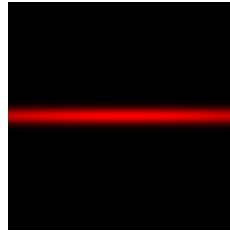
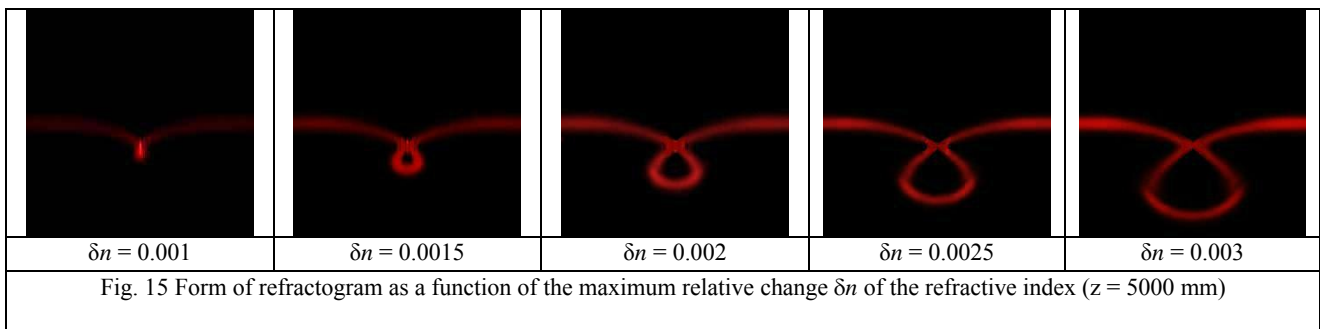
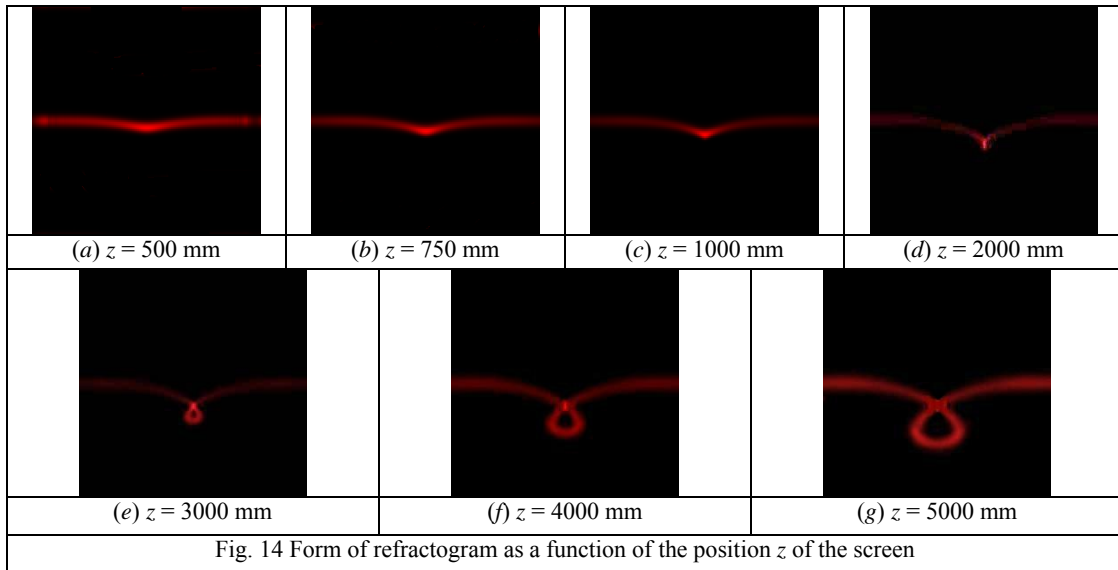


Fig. 13 Radiation at the entry to the inhomogeneity



3) The law of variation of the refractive index is

$$n = 1 + \delta n \exp\left(-\left(\frac{x}{ax}\right)^2 - \left(\frac{y-3}{aly}\right)^2\right),$$

which corresponds to a cylindrical inhomogeneity with a positive refractive index gradient.

The starting data like in the previous case.

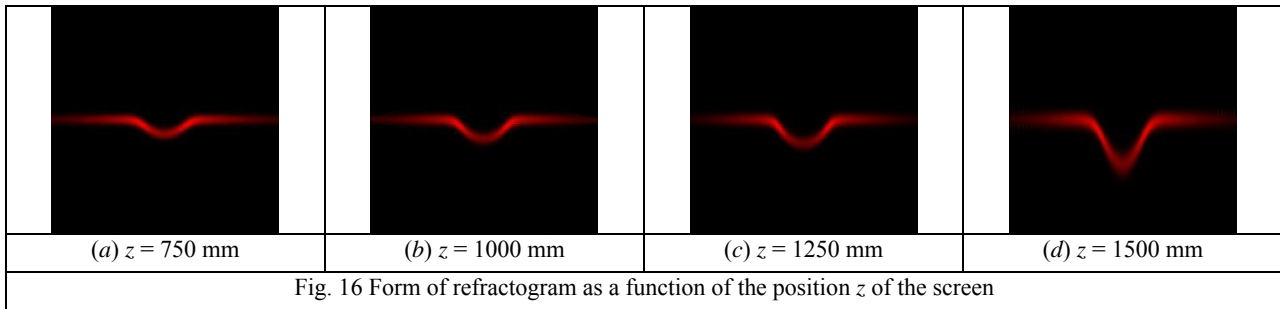


Fig. 16 Form of refractogram as a function of the position z of the screen

CONCLUSION

The laser refractography technique possesses all the advantages characteristic of laser measurements. These merits include the remotability and practically inertialess character of measurements and the possibility of taking nonperturbative and microscopic measurements. Laser refractography can be used to monitor stationary and fast processes (including thermal processes in liquids, gases, and plasmas), natural convection in liquids in the vicinity of heated or cooled bodies, and the processes of mixing of various liquids in process vessels and to diagnose temperature fields in boundary layers in heating and cooling applications and the fields of other physical quantities affecting the index of refraction.

The mathematical modeling of refraction patterns (refractograms) obtained in probing the media of interest with structured laser beams is a fundamental stage of quantitative diagnostics.

Geometrical-optics models of refractograms have been used to solve inverse problems on the recovery of the refractive index, temperature, and salinity of various media. However, where complex ray patterns are present or caustic surfaces formed in the medium, or else where diffraction effects must be taken into consideration, the geometrical-optics approach proves inconsistent, and so use should be made of wave methods. For this reason, the development of wave-equation-based refractogram processing algorithms is a high-priority task. The processing of refractograms in the domain of applicability of geometrical optics and in the Fresnel diffraction region involves problems associated with the need for substantial computational resources because of the presence of a fast oscillating function in the integrand.

To calculate this integral is very laborious and takes much time. In this connection, we have developed a special algorithm that increases the computation speed in comparison with direct computations in the *MathCAD* environment. At the base of the algorithm are numerical integration techniques, specifically the rectangle method whereby the domain of integration is divided into rectangular cells and the integral is replaced by a sum, owing to which the refractogram construction speed has increased by more than ten times.

Acknowledgments

This work was supported in part by the Ministry of Education and Science of the Russian Federation (State contract no. 14.740.11.0594.) and the Russian Foundation for Basic Research (project no. 10_08_00936a).

References

1. Fomin N.A. *Speckle photography for fluid mechanics measurements*. Springer, Berlin, 1998
2. Rinkevichyus B.S., Evtikhieva O.A., Raskovskaya I.L. *Laser Refractography*. Springer, New York, 2011, pp.201.
3. Esin M.V., Raskovskaya I.L., Rinkevichyus B.S., Tolkachev A.V. *3D Refractograms and Their Application in Diagnostics of Gradient Inhomogeneities*, 2012, published in Radiotekhnika i Elektronika, 2012, Vol. 57, No. 4, pp. 485–491.
4. Rinkevichyus B.S., Raskovskaja I.L., Tolkachev V.A. *Modern laser refractive techniques for flows investigation* //CD Room Proc. VI Minsk International Heat and Mass Transfer Forum. MIF 2008, Minsk, May 19-23, 2008,1-12pp